国立科博専報，(51), pp. 89–98 , 2016 年 3 月 28 日
Mem. Natl. Mus. Nat. Sci., Tokyo, (51), pp. 89–98, March 28, 2016

Chevkinite-bearing Tuffs from the Boso and Noto Peninsulas in Central Japan and from Primorye, Far East Russia

Koichi Momma*, Yukiyasu Tsutsumi, Takashi Sano, Ritsuro Miyawaki, Masako Shigeoka and Kazumi Yokoyama

Department of Geology and Paleontology, National Museum of Nature and Science,
4–1–1 Amakubo, Tsukuba, Ibaraki 305–0005, Japan
*E-mail: k-momma@kahaku.go.jp

Abstract. Specific tuffs including chevkinite-(Ce) or monazite-(Ce) were found in Oligocene to Miocene formations on the Boso and Noto peninsulas in central Japan. Monazite tuff was also found in Nezhino, Primorye, Far East Russia, where chevkinite-(Ce) was found in the river sands. The chemical composition of chevkinite-(Ce) from the Boso Peninsula is almost the same as that from the Noto Peninsula. Furthermore, ages of the chevkinite-bearing tuffs are around 23 Ma in both the tuffs. As chevkinite-(Ce) and monazite-(Ce) are very rare minerals in tuff, it is concluded that tuffs from the Boso and Noto peninsulas were derived from the same volcanic eruptions. The chevkinite-(Ce) collected from river sand from Nehino, Primorye, has chemical compositions similar to those mentioned above. Monazite-bearing tuff has ages similar to those from the Boso and Noto peninsulas. Hence, it is reasonable that the three tuffs were formed by the same or consanguineous volcanic eruption at around 23 Ma. These data will be important when we reconstruct the Japanese Islands before the opening of the Sea of Japan.
Key words: chevkinite, monazite, zircon, Sea of Japan

Introduction

Chevkinite-(Ce), $(Ce,La,Ca)_4(Ti,Fe^{3+},Fe^{2+},Mg)_5Si_4O_{22}$, is a rare mineral occurring as an accessory mineral in granitoid, pegmatite, tuff, and air-fall ash deposits (Mitchell, 1966; Izett *et al.*, 1968; Sokolova *et al.*, 2004; Platt *et al.*, 1987; Macdonald *et al.*, 2012). Tsutsumi *et al.* (2012) described chevkinite from the tuff in the Boso Peninsula. It is the first record of chevkinite-(Ce) in Asia found from tuff or ash deposits. They also described a monazite-bearing tuff closely associated with the chevkinite-bearing tuff. While monazite-(Ce) is a common accessory mineral in granitoid and high-grade metamorphic rock, it is rarely found in a tuff (Das *et al.*, 2009). The deposition age of these tuff or tuffaceous sandstones was around 23 Ma, just before the opening of the Sea of Japan.

To deduce the origin of the chevkinite-(Ce) in the Boso Peninsula, we recently collected tuffs and tuffaceous rocks that occur along the Sea of Japan from the Japanese Islands and Primorye,

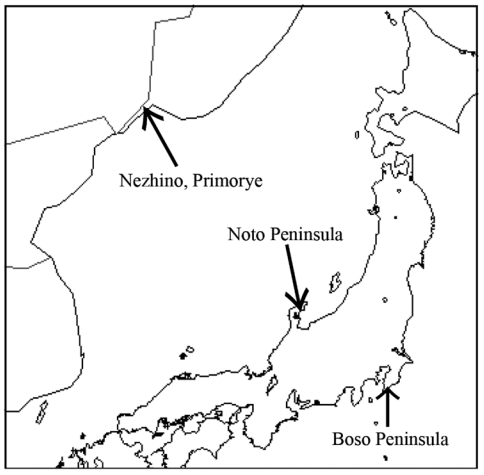

Fig. 1. Index map of the Boso and Noto peninsulas and Nejino of Primorye, Far East Russia.

Far East Russia (Fig. 1). In this paper, we describe the newly discovered chevkinite-(Ce) and monazite-(Ce) from tuffs and river sand in the Noto Peninsula and Primorye. Ages of these chevkinite-bearing or monazite-bearing tuffs provide important insight for the reconstruction of the Japanese Islands before the opening of the Sea of Japan.

Occurrence of chevkinite-bearing tuffs

In the Hegurinaka quarry, Boso Peninsula, more than ten tuff layers occur (Tsutsumi *et al.*, 2012). The heavy fractions, specific gravity >3.3, of all the tuffs were collected for more detailed analyses under Energy Dispersive Spectrometry. As an accessory mineral, zircon was found in all the samples. Among the tuffs, chevkinite-(Ce) is found as a common mineral in the heavy fractions of a tuff. Monazite-bearing tuff occurs associated with the chevkinite-bearing tuff (Tsutsumi *et al.*, 2012). Chevkinite-(Ce) is usually a euhedral crystal and occurs as a phenocryst ranging in size from 100 to 200 μm. The age of the chevkinite tuff was 23 Ma and was deposited in the deep-sea, showing that the constituent minerals were derived from the continental or island arc side.

As a possible source area of chevkinite-(Ce), we studied areas along the Sea of Japan, because Oligocene to Miocene volcanic rocks are abundant. We collected samples from the Noto Peninsula, Sado Island, Oga Peninsula, and Nagato areas in western Chugoku Province. Among the studied samples, chevkinite-(Ce) was found only in a dacitic tuff from the Goroku Formation in the Noto Peninsula (Fig. 2). According to the geological map presented by Yoshikawa *et al.* (2002), the geological age of the Goroku Formation is at around the boundary between the Oligocene to Early Miocene, which is similar to that from the Boso Peninsula. The Goroku Formation is composed mainly of dacite lava and volcaniclastic rocks. The chevkinite-bearing tuff collected is a thin layer with 15 cm thickness (Fig. 2). In addition to chevkinite-(Ce), the tuff contains a phenocryst of monazite-(Ce). The size of chevkinite-(Ce) is 100–200 μm, which is also the size of the chevkinite-(Ce) from the Boso Peninsula (Fig. 3). From the associated dacite lava, chevkinite-(Ce) was found only as an inclusion in zircon.

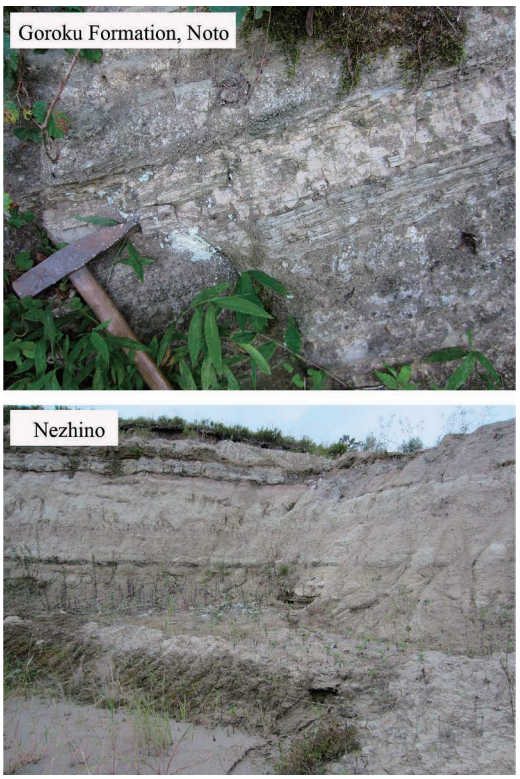

Fig. 2. Outcrop of Chevkinite-bearing tuff in the Goroku Formation from the Noto Peninsula and Monazite-bearing tuff from Nezino in Primorye, Far East Russia.

The Japanese Islands were located close to Primorye, Far East Russia, before the opening of the Sea of Japan at around 20 Ma. The eruption ages of the chevkinite tuffs from the Boso and Noto peninsulas were around 23 Ma. Therefore, as a possible occurrence of chevkinite-(Ce), we collected samples from Primorye, Far East Russia. In Primorye, Tertiary sediments are distributed locally along the Sea of Japan where most of the rocks are Pre-Tertiary granite and sedimentary rocks. The lava flow from the Oligocene occurs only in northern Primorye (Tatsumi *et al.*,

2000). Tuff and tuffaceous sandstone occur at the western part of Vladivostok. A tuffaceous sandstone sample was collected from a small quarry in Nezhino (Fig. 2). It contains a phenocryst of monazite-(Ce), but chevkinite-(Ce) is not observed. A sand sample was collected from a small river, the Nezhinka River, which cuts through the Tertiary sedimentary rocks. Several grains of chevkinite-(Ce) were found in the heavy fraction of the sand. They are usually euhedral in shape (Fig. 3), showing that they were derived from a nearby source, i.e. Tertiary sediments.

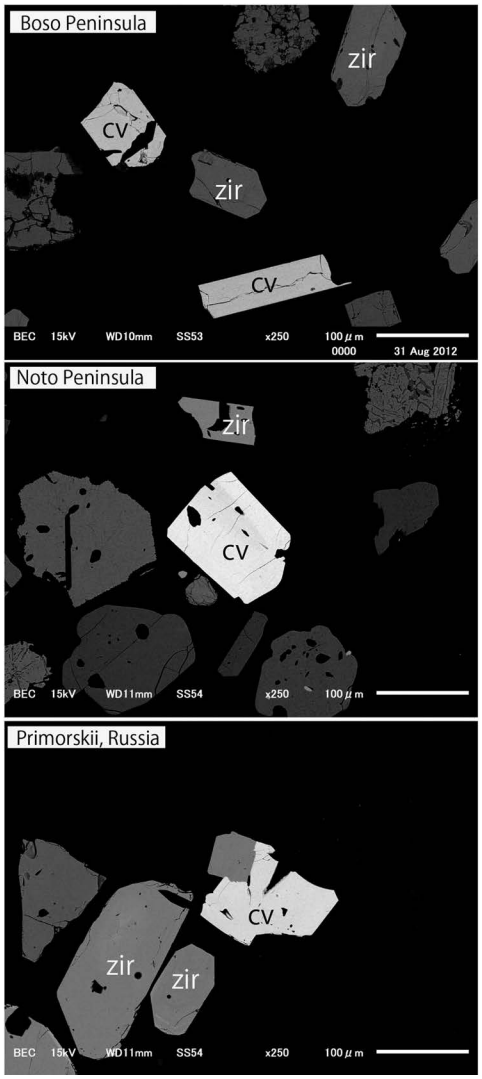

Fig. 3. Back-scattered image of the chevkinites from the Boso and Noto peninsulas and from Far East Russia. Mineral abbreviation: ch = chevkinite-(Ce), zir = zircon.

Chemical compositions of chevkinite-(Ce)

The chemical compositions of chevkinites from the Boso and Noto peninsulas and Primorye were analyzed by a JEOL electron microprobe analyzer. The accelerating voltage and current were 15 kV and 20 nA for chevkinite-(Ce), respectively. The following synthetic and natural materials were used as standards: wollastonite for Si and Ca; anatase for Ti; sillimanite for Al; Mg_2SiO_4 for Mg; Fe_2SiO_4 for Fe; rhodonite for Mn; albite for Na; YP_5O_{14} for Y; LaP_5O_{14} for La;

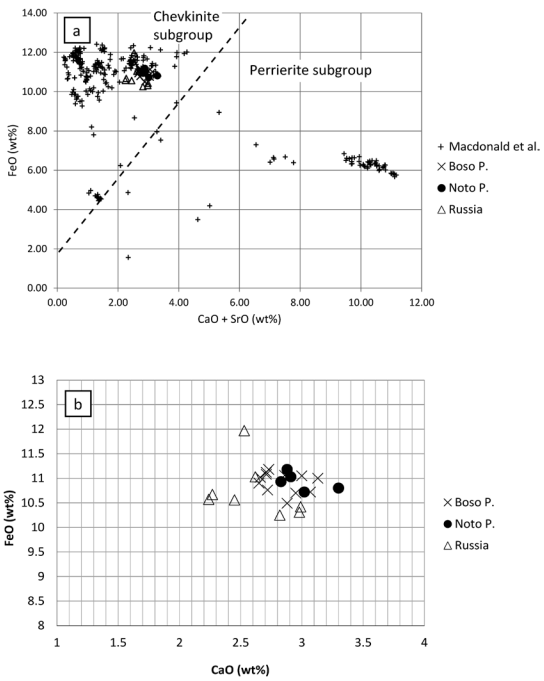

Fig. 4. An empirical FeO vs. (CaO + SrO) compositional variation of chevkinite-(Ce) from the Boso and Noto peninsulas and from Far East Russia. (a) Comparison of the present samples with chevkinite-group minerals from Russia and Mongolia (Macdonald *et al.*, 2012). (b) Enlarged plot of the present samples. The FeO wt% is total Fe expressed as Fe^{2+}.

Table 1. Chemical compositions of chevkinites from the Boso, Noto and from Primorye, Far East Russia.

Grain N.	SiO_2	TiO_2	Nd_2O_3	Al_2O_3	FeO	CaO	ThO_2	Y_2O_3	La_2O_3	Ce_2O_3	Pr_2O_3	Nb_2O_5	Sm_2O_3	Gd_2O_3	Dy_2O_3	Total
Chevkinite-(Ce) from the Boso Peninsula																
1	21.15	19.12	5.78	0.44	10.76	2.72	1.72	0.92	11.36	21.38	2.36	0.47	0.90	0.61	0.33	100.02
2	20.87	19.16	6.17	0.28	11.06	2.86	1.13	0.58	12.70	21.09	2.52	0.29	0.69	0.45	0.19	100.03
3	20.69	18.45	6.81	0.41	11.08	2.71	1.09	0.70	11.21	21.73	2.32	0.44	1.01	0.38	0.27	99.29
4	21.02	18.53	7.26	0.36	11.18	2.73	1.53	1.07	10.29	21.13	2.63	0.52	0.92	0.62	0.43	100.21
6	21.31	18.47	7.01	0.28	11.05	3.00	1.14	0.95	10.91	21.57	2.47	0.49	1.02	0.46	0.22	100.35
7	21.23	19.02	6.82	0.32	10.72	3.07	0.97	0.58	11.68	21.77	2.42	0.30	0.66	0.37	0.19	100.12
8	21.06	18.80	7.12	0.37	10.90	2.65	1.42	0.93	11.65	21.15	2.33	0.46	0.64	0.34	0.26	100.10
9	21.24	18.09	7.33	0.43	10.49	2.88	1.48	0.85	11.26	21.39	2.39	0.56	1.06	0.62	0.27	100.32
10	20.98	18.93	7.32	0.40	11.02	2.66	1.80	0.95	11.13	21.68	2.26	0.51	0.78	0.60	0.33	101.33
11	20.88	19.06	7.08	0.51	10.70	2.95	1.74	0.90	11.16	20.97	2.34	0.43	1.09	0.54	0.36	100.71
12	20.92	19.24	7.13	0.47	11.00	3.13	1.53	0.93	10.44	21.05	2.37	0.50	1.03	0.55	0.26	100.55
13	20.93	19.29	6.95	0.38	11.12	2.71	0.71	0.67	12.21	20.88	2.26	0.29	0.61	0.17	0.20	99.37
avg.	21.02	18.85	6.90	0.39	10.92	2.84	1.36	0.84	11.33	21.32	2.39	0.44	0.87	0.48	0.27	100.20
Chevkinite-(Ce) from the Noto Peninsula																
No.	SiO_2	TiO_2	Nd_2O_3	Al_2O_3	FeO	CaO	ThO_2	Y_2O_3	La_2O_3	Ce_2O_3	Pr_2O_3	Nb_2O_5	Sm_2O_3	Gd_2O_3	Dy_2O_3	Total
1	21.13	18.77	7.09	0.37	11.18	2.88	1.31	0.67	11.97	21.31	2.20	0.36	0.98	0.55	0.43	101.19
2	21.27	19.62	7.02	0.27	11.03	2.91	0.61	0.41	12.69	21.93	2.38	0.27	0.56	0.13	0.11	101.22
3	21.18	19.45	7.22	0.22	10.93	2.83	1.07	0.71	11.73	22.23	2.39	0.45	1.04	0.43	0.21	102.09
4	20.92	18.56	7.07	0.23	10.72	3.02	1.04	0.87	11.96	21.90	2.24	0.54	0.66	0.60	0.21	100.55
5	21.51	18.52	7.14	0.34	10.80	3.30	0.70	0.45	11.96	21.89	2.40	0.25	0.53	0.36	0.11	100.25
avg.	21.20	18.98	7.11	0.29	10.93	2.99	0.94	0.62	12.06	21.85	2.32	0.37	0.75	0.41	0.21	101.06
Chevkinite-(Ce) from Nejino, Primorye, Far East Russia																
No.	SiO_2	TiO_2	Nd_2O_3	Al_2O_3	FeO	CaO	ThO_2	Y_2O_3	La_2O_3	Ce_2O_3	Pr_2O_3	Nb_2O_5	Sm_2O_3	Gd_2O_3	Dy_2O_3	Total
1	21.19	19.18	7.55	0.38	10.25	2.82	0.74	0.62	12.18	21.02	2.45	0.32	0.63	0.32	0.23	99.87
2	20.85	15.51	6.85	0.07	11.97	2.53	0.86	0.52	11.37	22.45	2.06	2.56	1.02	0.62	0.39	99.62
3	21.24	18.27	7.70	0.27	11.03	2.62	0.89	0.41	11.53	21.86	2.22	0.28	0.76	0.67	0.22	99.97
4	21.01	18.27	7.42	0.30	10.67	2.27	0.85	0.57	12.42	22.20	2.47	0.36	0.68	0.51	0.37	100.37
5	21.14	17.59	7.50	0.30	10.56	2.45	0.96	0.60	11.19	22.18	2.39	0.44	0.75	0.37	0.41	98.84
6	20.75	18.76	7.46	0.31	10.57	2.24	1.11	0.68	11.92	22.50	2.45	0.32	0.61	0.17	0.30	100.15
7	21.17	19.11	7.19	0.43	10.31	2.98	0.65	0.47	12.43	21.86	2.40	0.13	0.49	0.26	0.29	100.17
8	19.31	19.74	6.38	0.37	10.42	2.99	0.40	0.42	12.96	22.64	2.39	0.48	0.65	0.58	0.18	99.90
avg.	20.83	18.30	7.26	0.30	10.72	2.61	0.81	0.54	12.00	22.09	2.35	0.61	0.70	0.44	0.30	99.86

CeP_5O_{14} for Ce; PrP_5O_{14} for Pr; NdP_5O_{14} for Nd; SmP_5O_{14} for Sm; GdP_5O_{14} for Gd; DyP_5O_{14} for Dy; $FeNb_2O_6$ for Nb; $MnTa_2O_6$ for Ta; UO_2 for U; and ThO_2 for Th. Chevkinite-(Ce) is mostly homogeneous under backscattered electron images (Fig. 3).

The chemical compositions of chevkinite-(Ce) from three localities are shown in Table 1. They are plotted in the CaO–FeO diagram shown by Macdonald & Bekin (2002). Although chevkinite-(Ce) shows a wide variation in CaO and FeO, chevkinite-(Ce) from the three localities are plotted in a narrow region in Fig. 4. Even in the more detailed diagram (Fig. 4b), chevkinites from the Boso Peninsula are plotted in the same narrow area as those from the Noto Peninsula. On the other hand, chevkinites from Nezhino, Primorye, are more variable than those from the Boso and Noto Peninsulas in the detailed figure. The difference is probably because the sandy grains in Nezhino were derived from some chevkinite-bearing tuffs in the drainage basin. The empirical formulae of chevkinite-(Ce) from Noto and Primorye, based on Si = 4 *apfu*, are $(Ce_{1.51}La_{0.84}Ca_{0.60}Nd_{0.48}Pr_{0.16}Y_{0.06}Sm_{0.05}Th_{0.04}Gd_{0.03}Dy_{0.01})_{\Sigma 3.78}(Ti_{2.69}Fe^{2+}_{1.00}Fe^{3+}_{0.73}Al_{0.06}Nb_{0.03})_{\Sigma 4.51}Si_{4.00}O_{21.04}$ and $(Ce_{1.55}La_{0.85}Ca_{0.54}Nd_{0.50}Y_{0.05}Sm_{0.05}Th_{0.04}Gd_{0.03}Dy_{0.02}Pr_{0.16})_{\Sigma 3.78}(Ti_{2.64}Fe^{2+}_{1.00}Fe^{3+}_{0.72}Al_{0.07}Nb_{0.05})_{\Sigma 4.49}Si_{4.00}O_{21.03}$, respectively.

X-ray Crystallography

There are two structure-types in chevkinite group minerals: chevkinite-type ($C2/m$) and perrierite-type ($P2_1/a$) structures. The two structure-types are topologically closely related and they

Table 2. Summary of single-crystal X-ray diffraction experiments of chevkinite-(Ce) from Noto and Primorye.

Sample	Noto	Primorye
Crystal Dimensions	0.080 × 0.070 × 0.040 mm	0.050 × 0.040 × 0.030 mm
Lattice Parameters	a = 13.4229(4) Å	a = 13.3921(4) Å
	b = 5.7444(2) Å	b = 5.7388(2) Å
	c = 11.0655(3) Å	c = 11.0504(3) Å
	β = 100.658(1)°	β = 100.653(1)°
	V = 838.50(4) Å^3	V = 834.63(4) Å^3
Space Group	$P2_1/a$ (#14)	
Z value	2	
Radiation	Mo$K\alpha$ (λ = 0.71075 Å, 50 kV, 24 mA)	
Structure Solution	Charge flipping (Superflip)	
Function Minimized	$\Sigma w(F_o^2 - F_c^2)^2$ where $w = 1/[\sigma^2(F_o^2) + (aP)^2 + bP]$ and $P = (\max(F_o^2,0) + 2F_c^2)/3$	
D_{calc}	4.550 g/cm^3	4.592 g/cm^3
μ(Mo $K\alpha$)	12.160 mm^{-1}	12.370 mm^{-1}
Temperature	25.0℃	23.0℃
$2\theta_{max}$	59.1°	60.1°
No. of Reflections Measured	9059	9509
Unique	2351 (R_{int} = 0.0460)	2442 (R_{int} = 0.0238)
Corrections	Lorentz-polarization	Lorentz-polarization
	Absorption	Absorption
	(trans. factors: 0.443–0.642)	(trans. factors: 0.577–0.708)
Weighting parameters, a, b	0, 5.6271	0.0198, 3.6504
$2\theta_{max}$ cutoff	59.1°	60.1°
No. Variables	173	173
$R1$ [$I > 2\sigma(I)$]	0.0329	0.0243
$R1$ (all reflections)	0.0408	0.0281
w$R2$ (all reflections)	0.0779	0.0581
Goodness of Fit Indicator	1.149	1.149
Final $\Delta\rho_{max}$ (e/Å^3)	2.05 e$^-$/Å^3	2.58 e$^-$/Å^3
Final $\Delta\rho_{min}$ (e/Å^3)	− 1.76 e$^-$/Å^3	− 1.63 e$^-$/Å^3

give similar powder X-ray diffraction patterns that are difficult to distinguish. To confirm the structure-type of the chevkinite samples from Noto and Primorye, single-crystal X-ray diffraction studies were carried out using a microdiffractometer (Rigaku VariMax with RAPID) equipped with a curved imaging plate with monochromatized Mo $K\alpha$ radiation. The Rigaku RAPID AUTO software package was used for processing of the diffraction data, including the application of a numerical absorption correction. The structure was solved by the charge flipping method using Superflip (Palatinus & Chapuis, 2007). The SHELXL-97 software package (Sheldrick, 2008) was used for structural refinement. Atomic scattering factors for neutral atoms and the coefficients for X-ray dispersion corrections were taken from the International Tables for Crystallography Volume C (Wilson, 1992). Summaries of the data collection and structure refinement are provided in Table 2. The single-crystal X-ray diffraction study of chevkinite-(Ce) from the Boso Peninsula was reported elsewhere (Miyawaki *et al.*, 2012).

The Noto and Primorye samples were confirmed to have the chevkinite-type unit cell. However, weak reflections violating extinction conditions of the $C2/m$ symmetry were observed and the true symmetry was revealed to be $P2_1/a$, which is a subgroup of $C2/m$. Although $P2_1/a$ is the same space group as the perrierite-type structure, the unit cells of chevkinite and perrierite are different, and the present samples have the chevkinite-type unit cell (Fig. 5). The refined structures were basically consistent with the previously reported $C2/m$ structures of chevkinite-(Ce). The symmetry lowering from $C2/m$ to its subgroup $P2_1/a$ is caused by small shifts of some of atoms from higher symmetry positions to lower symmetry positions. The refined structure parameters are listed in Tables 3 and 4. Based on the number of electrons in each site, which were

Table 3. Final atomic coordinates and displacement parameters (Å^2) of chevkinite-(Ce) from the Noto Peninsula.

Site	Occupancy	†No. of e$^-$	*x*	*y*	*z*	U_{eq}
*A*1	$Ce_{0.837(3)}Ca_{0.15}$	51.5	0.14381(2)	0.50559(5)	0.26605(3)	0.01579(11)
*A*2	$Ce_{0.807(3)}Ca_{0.15}$	49.9	0.06981(2)	−0.00897(6)	0.74053(3)	0.01752(11)
B	Fe	26	1/2	0	1/2	0.0132(2)
*C*1	$Ti_{0.795(19)}Fe_{0.205(19)}$	22.8	0.24883(6)	0.24920(13)	0.00009(8)	0.0112(2)
*C*2a	Ti	22	0	0	0	0.0122(2)
*C*2b	$Ti_{0.85(3)}Fe_{0.15(3)}$	22.7	1/2	0	0	0.0130(3)
Si1	Si	14	0.20111(9)	0.4994(2)	0.73113(11)	0.0107(3)
Si2	Si	14	0.14218(10)	0.0002(2)	0.45389(12)	0.0142(3)
O1A	O	8	0.0213(2)	0.7539(6)	0.1262(3)	0.0143(7)
O1B	O	8	0.0225(2)	0.2483(6)	0.1261(3)	0.0157(7)
O2	O	8	0.1465(2)	−0.0027(6)	0.9776(3)	0.0135(6)
O3	O	8	0.1860(3)	−0.0014(6)	0.5978(3)	0.0181(7)
O4	O	8	0.1520(2)	0.5014(5)	0.0104(3)	0.0142(6)
O5A	O	8	0.0707(3)	0.7769(8)	0.4059(4)	0.0311(10)
O5B	O	8	0.0772(3)	0.2328(7)	0.4051(4)	0.0290(9)
O6A	O	8	0.2260(3)	0.2649(6)	0.8145(3)	0.0155(7)
O6B	O	8	0.2301(3)	0.7340(6)	0.8143(3)	0.0163(7)
O7	O	8	0.0848(3)	0.5111(8)	0.6704(4)	0.0326(10)
O8	O	8	0.2294(4)	−0.0121(9)	0.3721(4)	0.0391(12)

Site	U_{11}	U_{22}	U_{33}	U_{23}	U_{13}	U_{12}
*A*1	0.01571(19)	0.01708(19)	0.01404(17)	0.00061(12)	0.00135(11)	0.00011(12)
*A*2	0.01198(19)	0.0288(2)	0.01203(18)	0.00018(14)	0.00277(11)	0.00011(13)
B	0.0153(4)	0.0154(5)	0.0081(4)	0.0006(3)	−0.0003(3)	0.0004(4)
*C*1	0.0115(3)	0.0125(4)	0.0094(4)	0.0001(3)	0.0012(3)	0.0002(3)
*C*2a	0.0121(5)	0.0141(6)	0.0108(5)	0.0001(4)	0.0031(4)	0.0002(4)
*C*2b	0.0127(5)	0.0135(6)	0.0125(6)	0.0003(4)	0.0010(4)	0.0000(4)
Si1	0.0124(5)	0.0101(6)	0.0095(6)	−0.0001(4)	0.0014(4)	0.0002(4)
Si2	0.0149(5)	0.0181(7)	0.0094(6)	−0.0004(5)	0.0019(4)	−0.0008(5)
O1A	0.0157(15)	0.0171(17)	0.0104(16)	0.0006(12)	0.0030(13)	0.0022(12)
O1B	0.0150(15)	0.0162(17)	0.0157(18)	−0.0010(13)	0.0022(13)	−0.0022(12)
O2	0.0129(14)	0.0139(16)	0.0147(15)	−0.0002(13)	0.0050(12)	0.0006(12)
O3	0.0217(16)	0.0205(18)	0.0111(15)	−0.0013(13)	0.0005(13)	−0.0020(14)
O4	0.0111(13)	0.0125(16)	0.0181(16)	−0.0007(13)	0.0007(12)	−0.0006(12)
O5A	0.038(2)	0.032(2)	0.021(2)	−0.0054(17)	−0.0015(17)	−0.0145(18)
O5B	0.032(2)	0.031(2)	0.024(2)	0.0054(17)	0.0028(17)	0.0128(17)
O6A	0.0244(18)	0.0101(15)	0.0110(16)	−0.0013(12)	0.0001(13)	0.0016(13)
O6B	0.0244(18)	0.0109(16)	0.0131(17)	−0.0026(13)	0.0021(14)	−0.0022(13)
O7	0.0164(17)	0.057(3)	0.022(2)	0.0011(19)	−0.0026(15)	0.0012(18)
O8	0.039(2)	0.059(3)	0.026(2)	0.002(2)	0.0231(19)	0.003(2)

Note: †Number of electrons in each site is calculated based on refined site occupancy.

calculated from the refined site occupancies, the *B* site is mainly occupied by Fe. The *C*2a site is occupied by Ti, and the *C*1 and *C*2b sites are occupied by Ti as well as a small amount of Fe. Bond distances and polyhedral volumes of these metal sites suggest that Fe at the *B* site is divalent, and Fe at other sites is largely trivalent.

Zircon age- LA-ICP-MS measurements

The zircon grains for analysis were hand-picked from heavy fractions of the chevkinite tuff from the Noto Peninsula and of the monazite-bearing tuffaceous sandstone from the Nezhino Quarry, Primorye, Far East Russia. Age analyses of zircons in the tuffs were carried out using the Laser Ablation Inductively Coupled Plasma Mass Spectrometer (LA-ICP-MS) installed at the National Museum of Nature and Science. The method was shown in detail by Tsutsumi *et al.* (2012).

Almost all zircons in the samples show rhyth-

Table 4. Final atomic coordinates and displacement parameters (Å^2) of chevkinite-(Ce) from Primorye.

Site	Occupancy	†No. of e$^-$	x	y	z	U_{eq}
*A*1	$Ce_{0.853(2)}Ca_{0.135}$	52.2	0.143607(17)	0.50851(4)	0.266318(19)	0.01348(7)
*A*2	$Ce_{0.819(2)}Ca_{0.135}$	50.2	0.069259(17)	−0.01413(4)	0.74018(2)	0.01460(8)
B	Fe	26	1/2	0	1/2	0.01176(16)
*C*1	$Ti_{0.799(14)}Fe_{0.201(14)}$	22.8	0.24791(4)	0.24861(9)	0.00000(5)	0.00987(16)
*C*2a	Ti	22	0	0	0	0.01104(18)
*C*2b	$Ti_{0.84(2)}Fe_{0.16(2)}$	22.7	1/2	0	0	0.0118(2)
Si1	Si	14	0.20050(7)	0.49894(15)	0.73113(8)	0.00924(18)
Si2	Si	14	0.14293(7)	0.00049(16)	0.45376(8)	0.01129(19)
O1A	O	8	0.02195(19)	0.7547(4)	0.1266(2)	0.0149(5)
O1B	O	8	0.02295(19)	0.2490(4)	0.1260(2)	0.0136(5)
O2	O	8	0.14622(18)	−0.0038(4)	0.9775(2)	0.0126(5)
O3	O	8	0.1859(2)	−0.0043(4)	0.5981(2)	0.0159(5)
O4	O	8	0.15181(18)	0.5022(4)	0.0105(2)	0.0136(5)
O5A	O	8	0.0687(2)	0.7815(5)	0.4051(3)	0.0242(6)
O5B	O	8	0.0799(2)	0.2347(5)	0.4051(3)	0.0225(6)
O6A	O	8	0.2246(2)	0.2632(4)	0.8142(2)	0.0148(5)
O6B	O	8	0.2324(2)	0.7328(4)	0.8144(2)	0.0143(5)
O7	O	8	0.0834(2)	0.5195(6)	0.6717(3)	0.0284(7)
O8	O	8	0.2319(3)	−0.0192(6)	0.3740(3)	0.0347(8)

Site	U_{11}	U_{22}	U_{33}	U_{23}	U_{13}	U_{12}
*A*1	0.01432(14)	0.01345(12)	0.01227(12)	0.00088(8)	0.00138(8)	0.00004(8)
*A*2	0.01030(14)	0.02386(14)	0.00978(12)	0.00022(9)	0.00224(8)	−0.00013(9)
B	0.0157(3)	0.0115(3)	0.0072(3)	0.0002(2)	−0.0001(2)	0.0005(2)
*C*1	0.0109(3)	0.0107(3)	0.0077(3)	0.00008(19)	0.00084(18)	0.00015(19)
*C*2a	0.0118(4)	0.0125(4)	0.0094(4)	0.0003(3)	0.0034(3)	0.0003(3)
*C*2b	0.0124(4)	0.0117(4)	0.0107(4)	−0.0007(3)	0.0008(3)	0.0002(3)
Si1	0.0108(4)	0.0084(4)	0.0083(4)	0.0001(3)	0.0015(3)	0.0006(3)
Si2	0.0134(4)	0.0130(4)	0.0074(4)	0.0003(3)	0.0019(3)	0.0001(3)
O1A	0.0146(12)	0.0171(12)	0.0131(12)	0.0024(9)	0.0027(9)	0.0026(9)
O1B	0.0150(12)	0.0156(12)	0.0107(11)	−0.0015(9)	0.0039(9)	−0.0029(9)
O2	0.0110(11)	0.0132(11)	0.0148(11)	−0.0003(9)	0.0052(9)	0.0010(9)
O3	0.0194(12)	0.0187(12)	0.0092(11)	0.0001(9)	0.0011(9)	−0.0001(10)
O4	0.0108(11)	0.0120(11)	0.0178(12)	0.0013(9)	0.0018(9)	0.0008(9)
O5A	0.0306(16)	0.0217(14)	0.0178(13)	−0.0028(11)	−0.0018(11)	−0.0111(12)
O5B	0.0249(14)	0.0223(14)	0.0191(14)	0.0051(11)	0.0007(11)	0.0088(11)
O6A	0.0236(13)	0.0105(11)	0.0097(11)	0.0017(9)	0.0016(9)	0.0021(9)
O6B	0.0226(13)	0.0093(11)	0.0104(11)	−0.0009(8)	0.0013(9)	−0.0007(9)
O7	0.0142(13)	0.049(2)	0.0198(14)	−0.0013(13)	−0.0033(10)	0.0011(13)
O8	0.0334(17)	0.052(2)	0.0250(16)	0.0061(14)	0.0210(14)	0.0081(15)

Note: †Number of electrons in each site is calculated based on refined site occupancy.

mic oscillatory and/or sector zoning on backscattered electron and/or cathodoluminescence images, which is commonly observed in igneous zircons. Fig. 6 shows Tera–Wasserberg concordia diagrams for all analyzed spots from zircons from the Noto Peninsula and Nezhino quarry obtained by LA-ICP-MS. All zircon age data of the sample from the Noto Peninsula (24 spots from 13 grains) cluster around ~25 Ma, and their weighted mean age yields 23.5 ± 0.7 Ma (95% conf.; MSWD = 0.97) (Fig. 6a). The zircons in the Nezhino tuffaceous sandstone indicate various ages around 25, 29, 70, 100, 180, 250, and 490 Ma. (Fig. 6b). The youngest age cluster consists of 2 data, 25.2 ± 0.8 Ma and 25.1 ± 0.9 Ma (1σ). Therefore the deposition age of the sample is thought to be younger than 25 Ma.

Discussion

Even though an enormous quantity of studies about volcanic ashes and tuffs in the Japanese

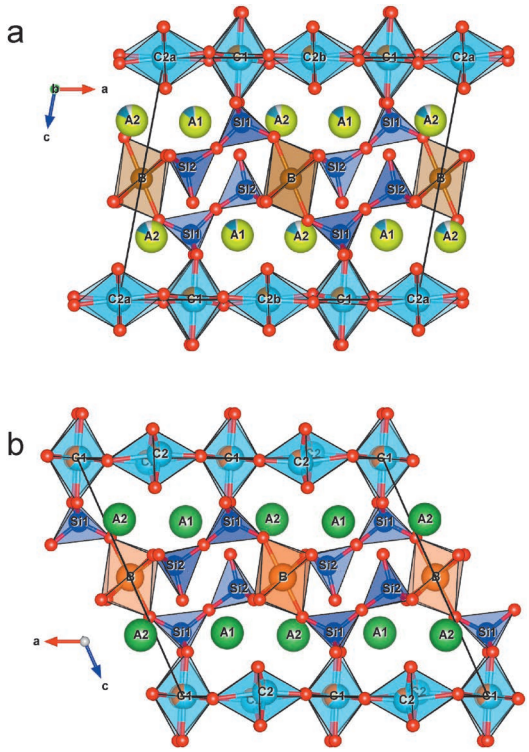

Fig. 5. Comparison of the structures of (a) chevkinite-(Ce) (this study, the Primorye sample) and (b) perrierite-(La) (Calvo & Faggiani, 1974). Although the two structures have the same topology of polyhedral arrangements, unit cells and positions of symmetry elements in the unit cells are different.

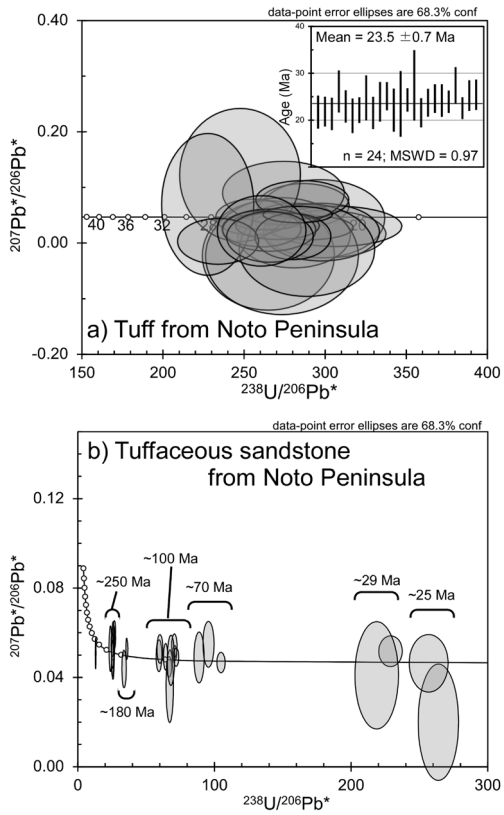

Fig. 6. Tera–Wasserburg U–Pb concordia diagrams and the age distribution plot of samples from the Noto Peninsula (a) and Nezhino quarry (b). $^{207}Pb^*$ and $^{206}Pb^*$ indicate radiometric ^{207}Pb and ^{206}Pb, respectively.

Islands have been conducted (*e.g.* Machida & Arai, 1992; Takahashi *et al.*, 2001), neither chevkinite nor monazite has previously been reported as a phenocryst. Such a rare mineral was found in a tuff layer from the Hegurinaka quarry, Boso Peninsula (Tsutsumi *et al.*, 2012). It is the first record from a tuff layer in East Asia. Such a rare mineral was found in the tuff from the Noto Peninsula and from sands in the river cutting through Tertiary sediments in Nezhino, Far East Russia. It is probable that the latter chevkinite-(Ce) was also derived from tuff layers because they are 100–200 μm in size and usually euhedral, similar to those from the Boso and Noto Peninsulas. Furthermore, chemical compositions are the same or similar to each other. And also, monazite as a phenocryst occurs in the tuffs from three localities. In addition to these identical natures, the ages of chevkinite tuffs from the Boso and Noto peninsulas and monazite tuff from the Nezhino Quarry are around 23 Ma, which is the end of the Oligocene. From these occurrences, it is concluded that the tuff was derived from the same volcanic eruption or consanguineous volcanic event. Tuff from the Boso Peninsula is a deep-sea deposit, whereas the other two tuffs are terrestrial deposits. Lava flows at the end of the Oligocene are common in the Noto Peninsula and are absent in the Nezhino area. The most possible story is that a volcano including chevkinite and/or monazite erupted around the Noto Peninsula and ash fall was carried to the ocean of Boso and the

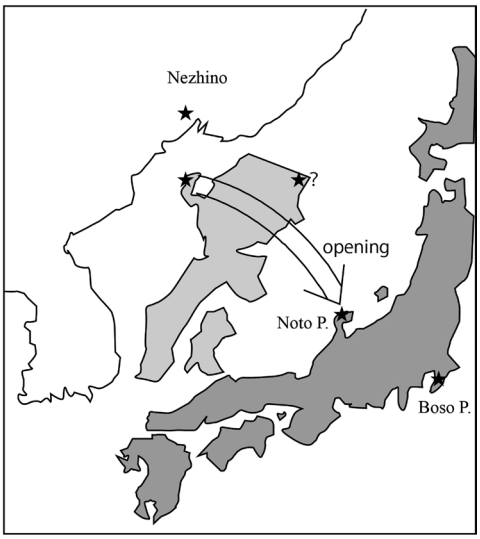

Fig. 7. Schematic illustration of the formation of the Sea of Japan.

inland area of Primorye, Far East Russia. Reconstruction models at the opening of the Sea of Japan have been presented by many authors. Fig. 7 shows one of the models where the Noto Peninsula is close to the Nezhino area. It is reasonable to conclude that a volcano in the Noto Peninsula provided ash to both the Boso Peninsula and the Nezhino area. Volcanism at the end of the Oligocene occurred along the Sea of Japan. Further study around the Noto Peninsula will contribute to the geotectonic reconstruction at the time of the opening of the Sea of Japan.

Acknowledgement

We would like to thank Dr. Sergei A. Kasatkin and Dr. Igor Chekryzhov to take us to the Nezhino quarries in Primorye, Far East Russia.

References

Black, L. P., S. L. Kamo, I. S. Williams, R. Mundil, D. W. Davis, R. J. Korsch & C. Foudoulis, 2003. The application of SHRIMP to Phanerozoic geochronology; a critical appraisal of four zircon standards. *Chemical Geology*, **200**: 171–188.

Calvo C. & R. Faggiani, 1974. A re-investigation of the crystal structures of chevkinite and perrierite. *American Mineralogist* **59**: 1277–1285.

Das K., K. Yokoyama, P. P. Chakraborty & A. Sarkar, 2009. Basal tuff contemporaneity of Chattisgarh and Khariar basins, based on new dates and geochemistry. *Journal of Geology,* **117**: 88–102.

Eggins, S. M., L. P. J. Kinsley & J. M. G. Shelley, 1998. Deposition and element fractionation processes of occurring during atmospheric pressure sampling for analysis by ICP-MS. *Applied Surface Science*, **129**: 278–286.

Hirata, T., 2002. *In-situ* precise isotopic analysis of tungsten using laser ablation multi-collector inductively coupled plasma mass spectrometry (LA-MC-ICP-MS) with time resolved data acquisition. *Journal of Analytical Atomic Spectrometry*, **17**: 204–210.

Izett, G. A. & R. E. Wilcox, 1968. Perrierite, chevkinite, and allanite in upper Cenozoic ash beds in the western United States. *American Mineralogist*, **53**: 1558–1567.

Ludwig, K. R., 2001. SQUID version: 1.03-A user's manual. Berkeley Geochronology Center Special Publication No. 2, pp. 19, Berkeley Geochronology Center, Berkeley, CA., USA.

Ludwig, K. R., 2003. User's manual for Isoplot 3.00. A geochronological toolkit for Microsoft Excel. Berkeley Geochronology Center Special Publication No. 4, pp 70, Berkeley Geochronology Center, Berkeley, CA., USA.

Machida H. & F. Arai, 1992. Atlas of Tephra in and around Japan. University of Tokyo press, Tokyo, Japan (In Japanese).

Macdonald, R. & H. E. Belkin, 2002. Compositional variation in minerals of the chevkinite group. *Mineralogical Magazine*, **66**: 1075–1098.

Macdonald, R., B. Bargiński, P. Kartashov, D. Zozulya & P. Dzierżanowski, 2012. Chevkinite-group minerals from Russia and Mongolia: new compositional data from metasomatites and ore deposits. *Mineralogical Magazine*, **76**: 535–549.

Mitchell, R. S., 1966. Virginia metamict minerals: perrierite and chevkinite. *American Mineralogist*, **51**: 1394–1405.

Miyawaki, R., S. Matsubara, K. Yokoyama, K. Momma, T. Sano, M. Shigeoka & K. Nishikubo, 2012. Chevkinite-(Ce) in tuff at Heguri, Boso Peninsula, Chiba Prefecture, Japan. *Bulletin of the National Museum of nature and Science*, *Series C*, **38**: 7–13.

Palatinus, L. & G. Chapuis, 2007. SUPERFLIP–a computer program for the solution of crystal structures by charge flipping in arbitrary dimensions. *Journal of Applied Crystallography*, **40**: 786–790.

Platt, R. G., F. Wall, C. T. Williams & A. R. Woolley, 1987. Zirconolite, chevkinite and other rare earth minerals from nepheline syenites and peralkaline granites and syenites of the Chilwa Alkaline Province, Malawi. *Mineralogical Magazine*, **51**: 253–263.

Sheldrick, G. M., 2008. A short history of SHELX. *Acta Crystallographica*, *A*, **64**: 112–122.

Sokolova E. V., F. C. Hawthorne, G. Della Ventura & P. M. Kartashov, 2004. Chevkinite-(Ce): Crystal structure and the effect of moderate radiation-induced damage on site-occupancy refinement. *Canadian Mineralogist*, **42**: 1013–1025.

Takahashi, N., T. Mitsuoka & K. Yokoyama, 2001. Correlation of tuffs occurring near the boundary between Tertairy and Quaternary in the central part of the Boso Peninsula and Choshi area, central Japan. *Memoirs of National Science Museum*, **37**: 21–34.

Tatsumi, Y., K. Sato & T. Sano, 2000. Transition from arc to intraplate magmatism associated with backarc rifting: evolition of the Sikhote Alin volcanism. *Geophysical Research Letters*, **27**: 1587–1590.

Tsutsumi, Y., K. Horie, T. Sano, R. Miyawaki, K. Momma, S. Matsubara, M. Shigeoka & K. Yokoyama, 2012. La-ICP-MS and SHRIMP ages of zircons in chevkinite and monazite tuffs from the Boso Peninsula, Central Japan. *Bulletin of the National Museum of Nature and Science, Series C*, **37**: 15–32.

Wilson, A. J. C., 1992. International Tables for Crystallography Volume C. Kluwer Academic Publishers, Dordrecht.

Yoshikawa, T., K. Kano, Y. Yanagisawa, M. Komazawa & E. Kikawa, 2002. Geological map of Japan 1:50,000, Suzumisaki, Noto-Geological Survey of Japan, AIST.

房総，能登，およびロシア極東沿海地方に分布するチェフキン石を含む凝灰岩

門馬綱一・堤　之恭・佐野貴司・宮脇律郎・重岡昌子・横山一己

房総半島，能登半島の漸新世から中新世の凝灰岩中より，チェフキン石を確認した．またロシア極東沿海地方のタフ中からモナズ石を確認し，近くの川砂からチェフキン石を確認した．房総と能登の凝灰岩のジルコン年代は日本海の拡大が始まる直前の約23 Maで，ほぼ同年代であり，ロシア極東沿海地方のモナズ石を含む凝灰質砂岩の年代も比較的近い．モナズ石やチェフキン石を含むタフ凝灰岩は非常に稀であるにも関わらず，これら3ヶ所の堆積物は時代的に近く，含まれるチェフキン石の化学組成もほぼ共通することから，これらの凝灰岩は同一噴火による堆積物である可能性が高く，日本海拡大前のプレート位置復元の鍵となる．